ISSN 1948-5204 (online)

World Journal of *Gastrointestinal Oncology*

World J Gastrointest Oncol 2022 May 15; 14(5): 947-1066

Published by Baishideng Publishing Group Inc

World Journal of Gastrointestinal Oncology

Contents

Monthly Volume 14 Number 5 May 15, 2022

CORRECTION

World Journal of Gastrointestinal Oncology

Monthly Volume 14 Number 5 May 15, 2022

Contents

ABOUT COVER

Editorial Board Member of *World Journal of Gastrointestinal Oncology*, Zilvinas Dambrauskas, MD, PhD, Professor, Department of Surgery and Institute for Digestive System Research, Lithuanian University of Health Sciences, Kaunas 50161, Lithuania. zilvinas.dambrauskas@lsmuni.lt

AIMS AND SCOPE

The primary aim of *World Journal of Gastrointestinal Oncology* (*WJGO*, *World J Gastrointest Oncol*) is to provide scholars and readers from various fields of gastrointestinal oncology with a platform to publish high-quality basic and clinical research articles and communicate their research findings online.

WJGO mainly publishes articles reporting research results and findings obtained in the field of gastrointestinal oncology and covering a wide range of topics including liver cell adenoma, gastric neoplasms, appendiceal neoplasms, biliary tract neoplasms, hepatocellular carcinoma, pancreatic carcinoma, cecal neoplasms, colonic neoplasms, colorectal neoplasms, duodenal neoplasms, esophageal neoplasms, gallbladder neoplasms, *etc*.

INDEXING/ABSTRACTING

The *WJGO* is now indexed in Science Citation Index Expanded (also known as SciSearch®), PubMed, PubMed Central, and Scopus. The 2021 edition of Journal Citation Reports® cites the 2020 impact factor (IF) for *WJGO* as 3.393; IF without journal self cites: 3.333; 5-year IF: 3.519; Journal Citation Indicator: 0.5; Ranking: 163 among 242 journals in oncology; Quartile category: Q3; Ranking: 60 among 92 journals in gastroenterology and hepatology; and Quartile category: Q3. The *WJGO*'s CiteScore for 2020 is 3.3 and Scopus CiteScore rank 2020: Gastroenterology is 70/136.

RESPONSIBLE EDITORS FOR THIS ISSUE

Production Editor: *Ying-Yi Yuan*; **Production Department Director:** *Xiang Li*; **Editorial Office Director:** *Ya-Juan Ma*.

NAME OF JOURNAL
World Journal of Gastrointestinal Oncology

ISSN
ISSN 1948-5204 (online)

LAUNCH DATE
February 15, 2009

FREQUENCY
Monthly

EDITORS-IN-CHIEF
Monjur Ahmed, Florin Burada

EDITORIAL BOARD MEMBERS
https://www.wjgnet.com/1948-5204/editorialboard.htm

PUBLICATION DATE
May 15, 2022

INSTRUCTIONS TO AUTHORS
https://www.wjgnet.com/bpg/gerinfo/204

GUIDELINES FOR ETHICS DOCUMENTS
https://www.wjgnet.com/bpg/GerInfo/287

GUIDELINES FOR NON-NATIVE SPEAKERS OF ENGLISH
https://www.wjgnet.com/bpg/gerinfo/240

PUBLICATION ETHICS
https://www.wjgnet.com/bpg/GerInfo/288

PUBLICATION MISCONDUCT
https://www.wjgnet.com/bpg/gerinfo/208

ARTICLE PROCESSING CHARGE
https://www.wjgnet.com/bpg/gerinfo/242

STEPS FOR SUBMITTING MANUSCRIPTS
https://www.wjgnet.com/bpg/GerInfo/239

ONLINE SUBMISSION
https://www.f6publishing.com

World Journal of Gastrointestinal Oncology

Submit a Manuscript: https://www.f6publishing.com

World J Gastrointest Oncol 2022 May 15; 14(5): 1014-1026

DOI: 10.4251/wjgo.v14.i5.1014

ISSN 1948-5204 (online)

ORIGINAL ARTICLE

Retrospective Study

Preoperative prediction of malignant potential of 2-5 cm gastric gastrointestinal stromal tumors by computerized tomography-based radiomics

Xue-Feng Sun, Hai-Tao Zhu, Wan-Ying Ji, Xiao-Yan Zhang, Xiao-Ting Li, Lei Tang, Ying-Shi Sun

Specialty type: Radiology, nuclear medicine and medical imaging

Provenance and peer review: Unsolicited article; Externally peer reviewed.

Peer-review model: Single blind

Peer-review report's scientific quality classification

Grade A (Excellent): A
Grade B (Very good): B, B
Grade C (Good): 0
Grade D (Fair): 0
Grade E (Poor): 0

P-Reviewer: Katayama Y, Japan; Tanaka T, Japan; Toyota S, Japan

Received: December 1, 2021
Peer-review started: December 1, 2021
First decision: December 27, 2021
Revised: December 29, 2021
Accepted: April 21, 2022
Article in press: April 21, 2022
Published online: May 15, 2022

Xue-Feng Sun, Hai-Tao Zhu, Wan-Ying Ji, Xiao-Yan Zhang, Xiao-Ting Li, Lei Tang, Ying-Shi Sun, Key laboratory of Carcinogenesis and Translational Research (Ministry of Education/Beijing), Department of Radiology, Peking University Cancer Hospital & Institute, Beijing 100142, China

Corresponding author: Ying-Shi Sun, MD, Chief Doctor, Key laboratory of Carcinogenesis and Translational Research (Ministry of Education/Beijing), Department of Radiology, Peking University Cancer Hospital & Institute, No. 52 Fucheng Road, Haidian District, Beijing 100142, China. sys27@163.com

Abstract

BACKGROUND

The use of endoscopic surgery for treating gastrointestinal stromal tumors (GISTs) between 2 and 5 cm remains controversial considering the potential risk of metastasis and recurrence. Also, surgeons are facing great difficulties and challenges in assessing the malignant potential of 2-5 cm gastric GISTs.

AIM

To develop and evaluate computerized tomography (CT)-based radiomics for predicting the malignant potential of primary 2-5 cm gastric GISTs.

METHODS

A total of 103 patients with pathologically confirmed gastric GISTs between 2 and 5 cm were enrolled. The malignant potential was categorized into low grade and high grade according to postoperative pathology results. Preoperative CT images were reviewed by two radiologists. A radiological model was constructed by CT findings and clinical characteristics using logistic regression. Radiomic features were extracted from preoperative contrast-enhanced CT images in the arterial phase. The XGboost method was used to construct a radiomics model for the prediction of malignant potential. Nomogram was established by combing the radiomics score with CT findings. All of the models were developed in a training group (n = 69) and evaluated in a test group (n = 34).

RESULTS

The area under the curve (AUC) value of the radiological, radiomics, and nomogram models was 0.753 (95% confidence interval [CI]: 0.597-0.909), 0.919

(95%CI: 0.828-1.000), and 0.916 (95%CI: 0.801-1.000) in the training group *vs* 0.642 (95%CI: 0.379-0.870), 0.881 (95%CI: 0.772-0.990), and 0.894 (95%CI: 0.773-1.000) in the test group, respectively. The AUC of the nomogram model was significantly larger than that of the radiological model in both the training group (Z = 2.795, P = 0.0052) and test group (Z = 2.785, P = 0.0054). The decision curve of analysis showed that the nomogram model produced increased benefit across the entire risk threshold range.

CONCLUSION

Radiomics may be an effective tool to predict the malignant potential of 2-5 cm gastric GISTs and assist preoperative clinical decision making.

Key Words: Gastrointestinal stromal tumors; Gastric gastrointestinal stromal tumors; Computed tomography; Malignant potential; Radiomics; Nomogram

Core Tip: The use of endoscopic surgery in gastrointestinal stromal tumors (GISTs) between 2 and 5 cm remains controversial considering the potential risk of metastasis and recurrence. Also, surgeons are facing great difficulties and challenges in assessing the malignant potential of 2-5 cm gastric GISTs. This study aimed to develop and evaluate computerized tomography-based radiomics for predicting the malignant potential of primary 2-5 cm gastric GISTs.

Citation: Sun XF, Zhu HT, Ji WY, Zhang XY, Li XT, Tang L, Sun YS. Preoperative prediction of malignant potential of 2-5 cm gastric gastrointestinal stromal tumors by computerized tomography-based radiomics. *World J Gastrointest Oncol* 2022; 14(5): 1014-1026

URL: https://www.wjgnet.com/1948-5204/full/v14/i5/1014.htm

DOI: https://dx.doi.org/10.4251/wjgo.v14.i5.1014

INTRODUCTION

Gastrointestinal stromal tumors (GISTs) are the most common mesenchymal tumors in the gastrointestinal tract and account for the majority of submucosal tumors[1,2]. They most frequently appear in the stomach (50%-60%) and small intestine (30%-35%) and rarely in the colorectum (5%) and esophagus (< 1%)[3,4]. GISTs are clinically heterogeneous with varying degrees of malignant potential. Therefore, preoperative evaluation of the biological behavior of GISTs is important for surgical decision making[3,5].

Endoscopic resection is an effective and safe method for treating gastric GISTs smaller than 2 cm[6-8]. Nevertheless, whether endoscopic surgery can be used for resecting gastric GISTs between 2 and 5 cm remains controversial considering the potential risk of metastasis and recurrence[6,9]. Also, surgeons are facing great difficulties and challenges in assessing the malignant potential of 2-5 cm gastric GISTs.

The frequencies of 2 to 5 cm gastric GISTs metastases with mitotic counts larger than 5/50 high-power fields (HPFs) and smaller than 5/50 HPFs are 16% and 1.9%, respectively[10]. Based on mitotic counts, several risk stratification systems have been proposed to assess the recurrence risk after complete resection of primary GISTs[10-12]. Gastric GISTs are generally associated with a better prognosis than non-gastric GISTs[10]. The modified National Institutes of Health (NIH) criteria classify GISTs into four categories (very low, low, intermediate, and high risk) according to tumor location, mitotic count, tumor size, and tumor rupture. The modified NIH criteria have become a commonly accepted risk stratification tool for GISTs due to their important value in assessing prognosis after operation[13-15]. However, these criteria are only postoperatively applied as the mitosis count of the specimen available after excision is a significant criterion factor.

Preoperative prediction of the malignant potential and prognosis of these GISTs is crucial for clinical decision-making. Preoperative biopsy is a common method for determining the characteristics of suspected lesions. Yet, this method has several disadvantages, such as the lack of adequate tissue for fine-needle biopsy, the possible failure to obtain mitosis counts with improper sampling, or the underestimation of mitotic grades, which increase the difficulty of response evaluation during follow-up. On the other hand, with the recent remarkable development of imaging technology, non-invasive real-time imaging tools, such as computerized tomography (CT), magnetic resonance imaging, and endoscopic ultrasound (EUS), have been increasingly applied for assessing the potential malignancy and prognosis of a variety of tumors including GISTs. For example, Chen *et al*[13] indicated that CT features are more useful than EUS features for predicting mitotic counts. Therefore, exploring the association between CT

features and GIST risk stratification may influence the surgical treatment decision for 2-5 cm gastric GISTs. Nevertheless, subjective assessments may overlook abundant information hidden in the images and may be limited by overreliance on observers' experience.

As a combination of texture analysis and machine learning methods, radiomics has been widely used in the field of assisted tumor diagnosis, staging, and prognosis prediction[16,17]. Many studies have indicated that radiomics features can be used to comprehensively assess the biological behavior of malignant cells, improving the accuracy of diagnosis, prognosis, and prediction[18-20]. Radiomics has also been used to preoperatively predict the malignant potential of GISTs[21]. However, the study on 2-5 cm gastric GISTs has not yet been reported.

The aim of the current study was to propose a radiomics model for predicting the malignant potential of 2-5 cm gastric GISTs by preoperative enhanced CT images. The method may be helpful for preoperative design of individualized treatment strategy for patients with 2-5 cm gastric GISTs.

MATERIALS AND METHODS

Subjects

This retrospective study was approved by our institutional review board, and patient's informed consent was waived. A total of 695 gastric GIST patients with histologically confirmed 2-5 cm gastric GISTs who were treated at our hospital were consecutively enrolled between January 2010 and December 2019. The inclusion criteria were the following: Patients who underwent surgery for primary gastric GISTs with curative intent, patients who underwent standard contrast-enhanced CT less than 15 d before surgical resection; patients with complete clinicopathologic data; and patients with a tumor size of 2-5 cm.

The exclusion criteria were: Patients who received imatinib therapy or other tyrosine kinase inhibitor as a neoadjuvant therapy before surgery; and patients who had tumor rupture before or during surgery.

Finally, 592 patients were excluded due to the above reasons, and 103 patients were included in this study (48 males and 55 females; mean age, 58.31 ± 9.20 years). The included patients were randomly divided into a training group (n = 69) and a test group (n = 34) in a portion of 2:1 ratio with equal proportions of positive and negative samples. The inclusion and exclusion criteria are shown in Figure 1.

CT imaging

Contrast-enhanced CT examinations were performed using one of the following CT scanners: GE LightSpeed VCT (n = 62) or GE Discovery CT750 HD (n = 41). All patients were fasted for at least 8 h before the examination. They were given 6 g of gas production powder orally before the examination to ensure adequate expansion of the gastric cavity. CT images were obtained during breath holding. Both scanners used 5 mm slice thickness, 5 mm slice increment, 0.9 pitch, 120 kV tube voltage, and 300 mA tube current.

Contrast-enhanced scanning was performed for all subjects. They were intravenously administered 70-100 mL of a nonionic contrast agent (iohexol, 300 mg I/L; General Electric) at a rate of 2.5-3.5 mL/s. For the arterial phase, a delay time of 30 s was used. Venous phase and delayed phase scanning were performed 60 s and 120 s after contrast agent injection.

Axial, sagittal, and coronal multiplanar reconstructions images were obtained with a reconstruction thickness of 2-5 mm. CT images were sent to the picture archiving and communication system (PACS) for interpretation at the workstations.

CT findings and radiological model

Two radiologists with 14 years and 5 years of experience in abdominal imaging independently reviewed all images. In case of disagreement, the two readers jointly reviewed the findings to reach a consensus for further analysis. The radiologists were blinded to the pathological data.

The following CT findings were recorded: tumor size (cm), location (cardiac region, fundus, body, or antrum), necrosis (present or absent), ulceration (present or absent), calcification (present or absent), growth pattern, tumor contour (irregular or regular), and tumor margin (poorly or well defined). Tumor size was defined as the maximal diameter on the transverse, coronal, or sagittal plane. Ulceration was defined as a focal mucosal defect/indentation filled with air or fluid or when contrast material was found on the endoluminal surface of the lesion. Growth patterns were classified as endoluminal, exophytic, or mixed. The tumor contour was considered as either regular/round/ovoid or irregular/lobulated. The mean CT value (Hounsfield unit) was measured in the plain phase, arterial phase, venous phase, and delayed phase. Univariate analysis was used to select useful CT findings. A radiological model was constructed by the selected CT findings using backward logistic regression.

Tumor delineation

The regions of GISTs were manually delineated by a junior radiologist (with 5 years of experience in abdominal imaging diagnosis) with the 3D Slicer (version 4.8.1) in the axial direction. A senior

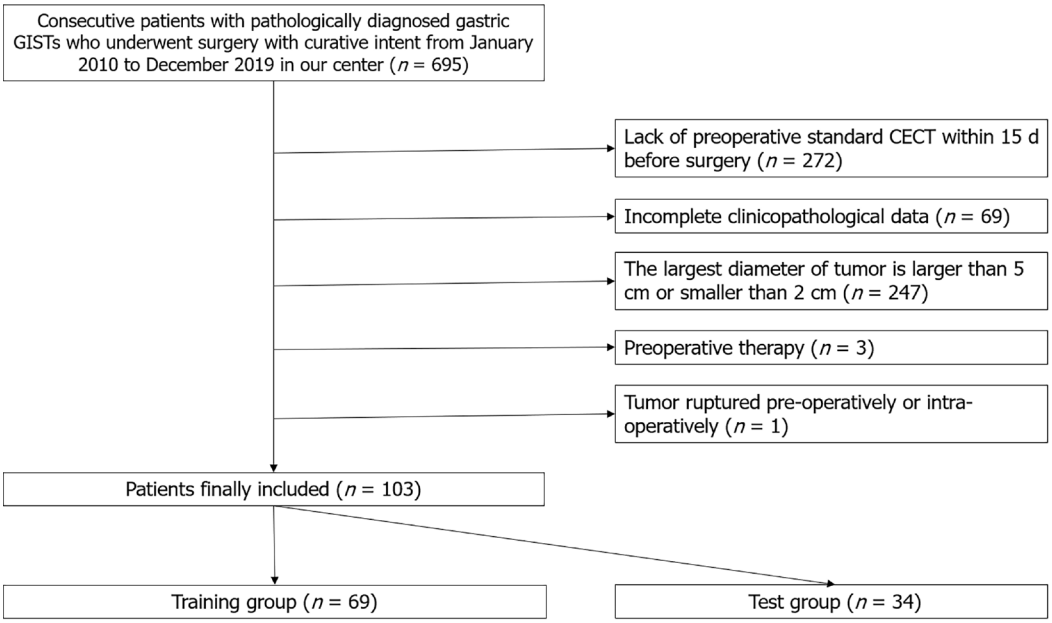

DOI: 10.4251/wjgo.v14.i5.1014

Figure 1 Flowchart of patient inclusion and exclusion. CECT: Contrast-enhanced computerized tomography; GISTs: Gastrointestinal stromal tumors.

radiologist (with 14 years of experience) evaluated the delineations and made modifications if needed. Delineation was performed on each slice of CT images from the artery phase to cover the whole tumor. Both radiologists were blinded to the risk classification of patients. One example is shown in Figure 2.

Feature extraction

Pyradiomic (version 3.0.1) was used to extract 851 features from the region of interest (ROI), including 14 shape features, 18 first-order features, 75 second-order (texture) features (24 gray level co-occurrence matrix features, 14 gray level dependence matrix features, 16 gray level run length matrix features, 16 gray level size zone matrix features, 5 neighboring gray-tone difference matrix features), and their 8 kinds of wavelet transforms ([18 + 75] × 8 + 18 + 75 + 14 = 851).

Low-grade and high-grade malignant potential

According to the NIH–modified criteria[11], mitotic counts > 5/50 HPFs were categorized into high grade, and mitotic counts < 5/50 HPFs were categorized into low grade. Then patients were divided into the very low/low-risk group (low-grade malignant potential group, n = 82) and the moderate/high-risk group (high-grade malignant potential group, n = 21). Low grade was labeled 0, and high grade was labeled 1 as the ground truth for training and test.

Radiomics model

First, a t-test examination was performed to compare all the features between the high-grade and low-grade groups. The features with $P > 0.05$ were removed. Second, the correlation was calculated between each pair of the features. If the absolute value of correlation was > 0.5, the feature with a smaller T value in the t-test was removed. Third, the XGboost algorithm was used to construct a model with remaining features and ground truth.

Due to the small sample size, the maximum estimator number and the maximum depth were set to 3 to avoid overfitting. A 3-fold cross-validation was used to determine the optimal tree number and depth. After cross-validation, the whole training group was trained again by the fixed hyperparameter to obtain the predictive model. A radiomics score was generated by the model for each patient. Finally, the model was assessed in the test group.

Nomogram model

Logistic regression was performed in the training group to classify high-grade and low-grade by combining radiomics scores with CT findings. Nomogram was used to visualize the combination of radiomics score and the selected CT findings. A risk score was generated by the nomogram and evaluated in the test group.

Decision curve of analysis

Decision curve of analysis (DCA) was performed to study the benefit of radiomics model. Net benefit was calculated by subtracting the proportion of all patients who were false positive from the proportion

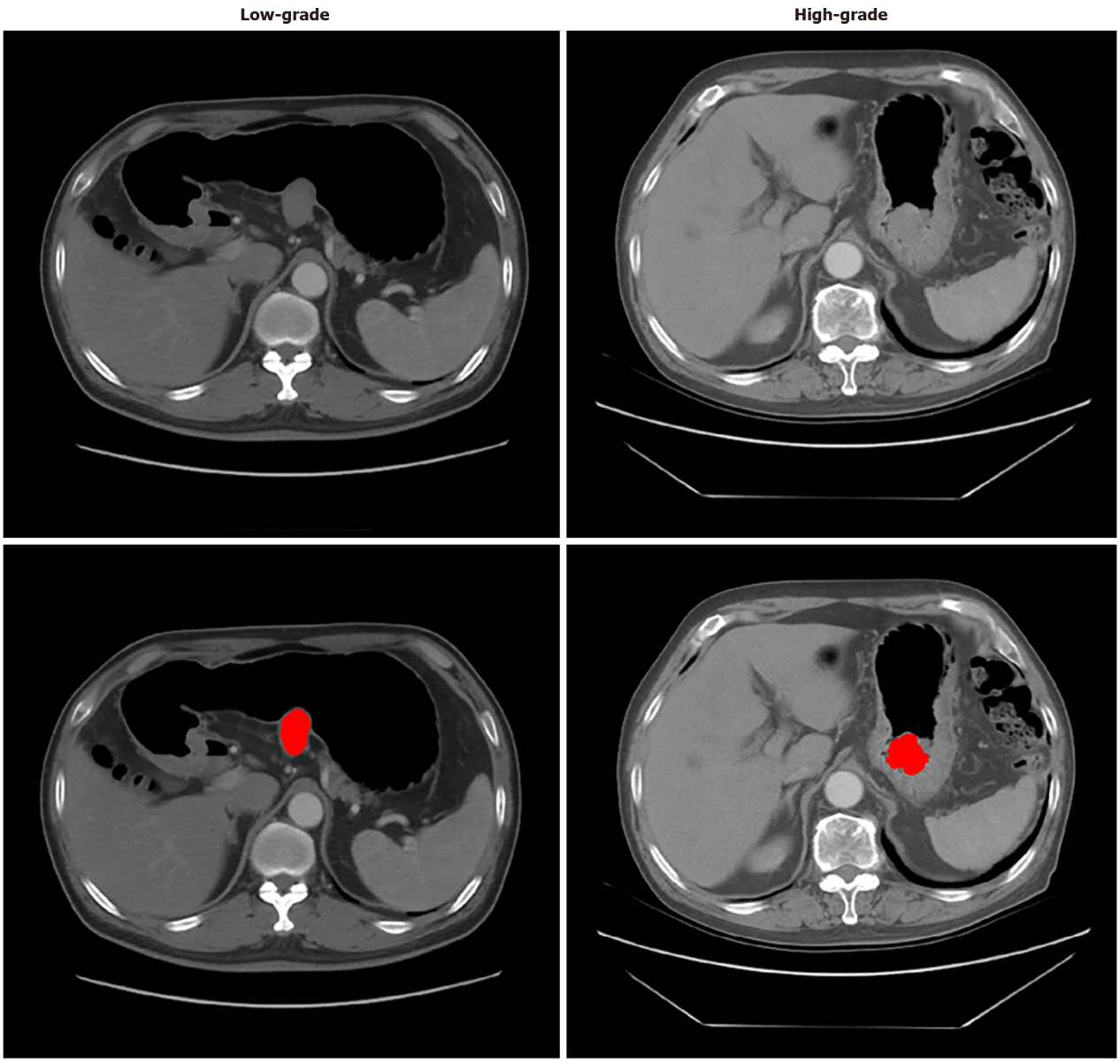

DOI: 10.4251/wjgo.v14.i5.1014

Figure 2 Two examples of computerized tomography images and tumor delineation (red color). The left one was proven low-grade malignant potential, and the right one was proven high-grade malignant potential by pathological analyses with mitotic counts.

of those who were true positive, weighted by the relative harm of forgoing treatment compared with the negative consequences of unnecessary treatments. Standardized net benefit scaled the net benefit into the range between 0 and 1. The relative harm was the ratio of the harm of false positive harm to false negative harm.

Statistical analyses

Independent samples *t*-test was used to compare the continuous variables in the low and high malignant potential groups. Chi-squared test or Fisher's exact test was applied for categorical variables. Receiver operating characteristic (ROC) curves were used to evaluate the predictive model. The cutoff value between low grade and high grade was selected by maximizing the Youden index (sensitivity + specificity-1). The area under the curve (AUC) was compared by the DeLong method.

RESULTS

Patient characteristics

The clinical characteristics and CT findings between the low-grade and high-grade malignant potential groups are analyzed in Table 1. In univariate analyses, tumor diameter, necrosis, ulceration, tumor

Table 1 Patients' characteristics between low-grade and high-grade malignant potential groups

Characteristics	Low-grade, *n* = 82	High-grade, *n* = 21	*t* or χ^2 value	*P* value
Age in year	58.57 ± 8.90	57.28 ± 10.47	0.570	0.570
Sex, *n* (%)			0.354	0.552
Male	37 (45.1)	11 (52.4)		
Female	45 (59.9)	10 (47.6)		
Largest diameter	32.66 ± 8.77	38.76 ± 9.09	2.824	0.006[a]
Location, *n* (%)			2.109	0.550
Cardia	2 (2.4)	0 (0)		
Fundus	40 (48.8)	12 (57.1)		
Body	28 (34.1)	8 (38.1)		
Antrum	12 (14.6)	1 (4.8)		
Growth patterns, *n* (%)			2.196	0.334
Endoluminal	39 (47.6)	11 (52.4)		
Exophytic	24 (29.3)	3 (14.3)		
Mixed	19 (23.2)	7 (33.3)		
Contour, *n* (%)			4.646	0.031[a]
Regular	56 (68.3)	9 (42.9)		
Irregular	26 (31.7)	12 (57.1)		
Margin, *n* (%)			5.645	0.018[a]
Well-defined	67 (81.7)	12 (57.1)		
Poorly	15 (18.3)	9 (42.9)		
Necrosis, *n* (%)			4.268	0.039[a]
Absent	48 (58.5)	7 (33.3)		
Present	34 (41.5)	14 (66.7)		
Calcification, *n* (%)			0.630	0.427
Absent	75 (91.5)	18 (85.7)		
Present	7 (8.5)	3 (14.3)		
Ulceration, *n* (%)			7.823	0.005[a]
Absent	67 (81.7)	11 (52.4)		
Present	15 (18.3)	10 (47.6)		
Plain CT value	34.65 ± 37.92	31.10 ± 13.23	0.421	0.674
Arterial phase CT value	63.70 ± 36.50	59.81 ± 18.58	0.471	0.639
Venous phase CT value	71.78 ± 35.76	63.43 ± 17.32	1.035	0.303
Delayed phase CT value	73.65 ± 34.96	66.14 ± 14.39	0.960	0.339

[a]$P < 0.05$.

Independent samples *t*-test was applied in continuous variables. χ^2 test was applied for categorical variables. CT: Computerized tomography.

margin, and tumor contour significantly differed between the different risk stratification groups (all $P < 0.05$). No significant differences were found in other subjective features between the two groups, including tumor location, growth pattern, calcification, density, and the degree of enhancement in each phase of CT between the different risk stratification groups (all $P \geq 0.05$). Table 2 compares the basic characteristics between the training and the test group. Moreover, there was no significant difference in age, sex, and ground truth between the two groups.

Table 2 Patients' characteristics between the training group and the test group

Characteristics	Training, *n* = 69	Test, *n* = 34	*t* or χ^2 value	*P* value
Age in year	58.30 ± 9.02	58.32 ± 9.71	0.01	0.992
Sex, *n* (%)			0.004	0.948
Male	32 (53.6)	16 (52.9)		
Female	37 (46.4)	18 (47.1)		
Ground truth, *n* (%)			0.001	0.972
Low-grade	55 (79.7)	27 (79.4)		
High-grade	14 (20.3)	7 (20.6)		

Prediction by radiological model

A radiological model was constructed by backward logistic regression using five selected CT findings including tumor diameter, necrosis, ulceration, tumor margin, and tumor contour. Two features were retained in the final model, including the largest diameter (P = 0.032; odds ratio [OR] = 1.082, 95% confidence interval [CI]: 1.007-1.163) and ulceration (P = 0.061; OR = 3.618, 95%CI: 0.943-13.876). The performance of this radiological model is summarized in Table 3. The AUC value was 0.753 (95%CI: 0.597-0.909) for the training group and 0.642 (95%CI: 0.379-0.870) for the test group.

Prediction by radiomics model

After the removal of features *via* *t*-test and correlation, 13 features remained. XGboost method selected four features by three-fold cross-validation with an optimal learning rate of 0.03. The four selected features and their importance were: gray-level nonuniformity (wavelet-HHH glszm feature type) with an importance of 0.703, mean absolute deviation (wavelet-HHH first-order feature type) with an importance of 0.154, small dependence low gray level emphasis (wavelet-LHH gldm feature type) with an importance of 0.098, and maximum (wavelet-LHL_firstorder) with an importance of 0.045. Figure 3 shows the two trees (estimators) for classification. The radiomics score is the summation of the scores from the two trees. The prediction results by radiomics score are summarized in Table 3. The AUC of the prediction by radiomics model was 0.919 (95%CI: 0.828-1.000) for the training group and 0.881 (95%CI: 0.772-0.990) for the test group.

Prediction by nomogram model

Three CT findings were selected by linear regression to combine with the radiomics score above, including necrosis, calcification, and ulcer. Nomogram was plotted as shown in Figure 4. The prediction result by the risk calculated from the nomogram is also summarized in Table 3. The AUC predicted by the nomogram model was 0.916 (95%CI: 0.801-1.000) for the training group and 0.894 (95%CI: 0.773-1.000) for the test group. The ROC curves of the radiological model, radiomics model, and nomogram model were plotted as shown in Figure 5. The AUC of the nomogram model was significantly larger than that of the radiological model in both the training group (Z = 2.795, P = 0.0052) and the test group (Z = 2.785, P = 0.0054).

DCA

Figure 6 shows the result of DCA. The y-axis measured the net benefit. The red line represents the prediction by the nomogram model. The blue line represents the assumption that all patients have high-grade malignant potential GISTs. The horizontal green line represents the assumption that all patients have low-grade malignant potential GTSTs. A 95%CI (dashed line) was determined by 1000 bootstraps. The results showed that the nomogram model produced increased benefit across the whole risk threshold range.

DISCUSSION

GISTs initiate from very early forms of Cajal cells in the gastrointestinal tract wall[22]. GISTs have complex and unpredictable biological behavior, with KIT or platelet-derived growth factor receptor A (PDGFRA) being the main pathogenetic pathways[23]. Up-to-date clinical practice guidelines suggest that the standard treatment for localized GISTs is complete surgical excision. R0 excision (microscopically negative margins) is the goal, especially for patients with a high risk of recurrence. According to recent studies, when surgery is technically challenging (rectum, duodenum, and gastroesophageal junction surgeries) and preoperative cytoreduction may facilitate tumor R0 excision, preoperative imatinib should be considered. Imatinib is currently the first-line molecular targeted drug for the

Table 3 The sensitivity, specificity, positive predictive value, and negative predictive value of the prediction by radiological model, radiomics model, and nomogram model with their 95% confidential intervals

Model	AUC	Sensitivity	Specificity	PPV	NPV
Radiological training	0.753 (0.597-0.909)	42.9 (17.7-71.1)	96.4 (87.5-99.6)	75.0 (34.9-96.8)	86.9 (75.8-94.2)
Radiological test	0.642 (0.379-0.870)	71.4 (29.0-96.3)	66.7 (46.0-83.5)	35.7 (12.8-64.9)	90.0 (68.3-98.8)
Radiomic training	0.919 (0.828-1.000)	92.9 (66.1-99.8)	80.0 (67.0-89.6)	54.2 (32.8-74.4)	97.8 (88.2-99.9)
Radiomic test	0.881 (0.772-0.990)	100.0 (59.0-100.0)	66.7 (46.0-83.5)	43.7 (19.8-70.1)	100.0 (81.5-100.0)
Nomogram training	0.916 (0.801-1.000)	85.7 (57.2-98.2)	90.9 (80.0-97.0)	70.6 (44.0-89.7)	96.2 (86.8-99.5)
Nomogram test	0.894 (0.773-1.000)	100.0 (59.0-100.0)	66.7 (46.0-83.5)	43.7 (19.8-70.1)	100.0 (81.5-100.0)

AUC: Area under the curve; NPV: Negative predictive value; PPV: Positive predictive value.

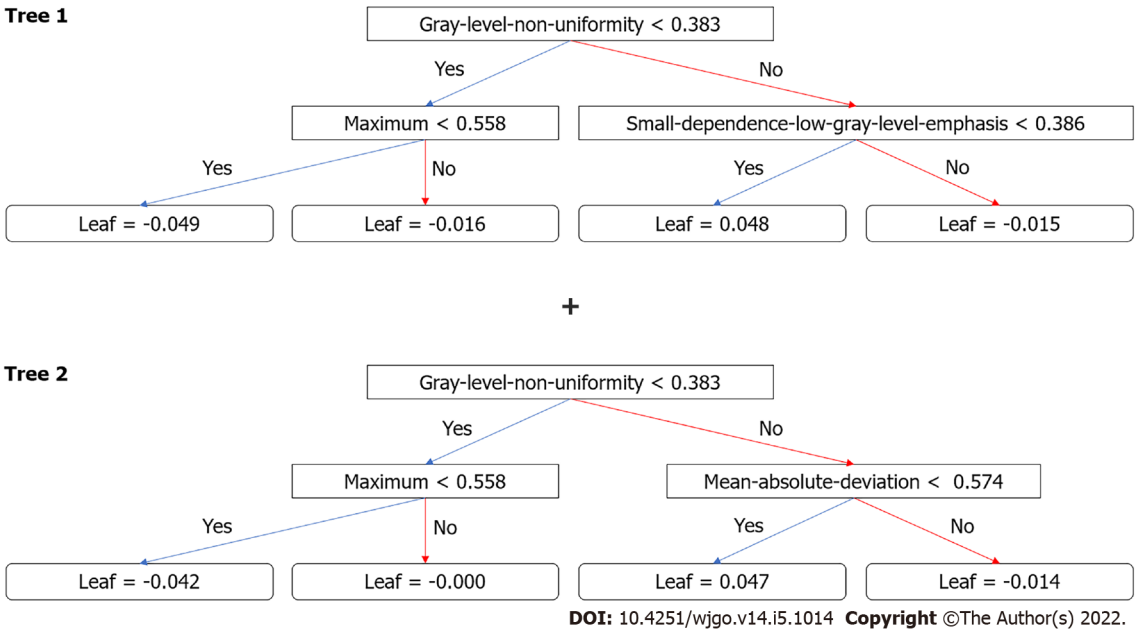

DOI: 10.4251/wjgo.v14.i5.1014

Figure 3 Decision trees generated by XGboost method for classification. Radiomics score is the sum of the scores from the two trees.

treatment of GISTs, and can be used in combination with KIT and PDGFRA[24]. The current guidelines recommend more than 3 years of adjuvant treatment for high-risk GISTs patients[25]. Patients with low malignant potential (low and very low risk) generally have a good prognosis and do not require further adjuvant imatinib therapy[26-28]. The majority of GISTs < 2 cm usually have risk of metastasis and their mitotic counts are < 5 per 50 HPFs in general. Conversely, for GISTs between 2-5 cm, there is a 10-fold difference in metastasis frequency between low- and high-mitosis groups[10]. According to the current diagnosis and treatment paradigm, individualized preoperative prediction of recurrence is particularly important for 2-5 cm GISTs. While the modified NIH consensus criteria are frequently used to estimate the risk of recurrence, the key criteria are only postoperatively accessible. A biopsy may provide preoperative estimation. However, a core needle biopsy may not provide an accurate mitotic count and a full-scale malignant potential assessment of the tumor. Therefore, a new robust risk assessment standard is needed.

Contrast-enhanced CT is the standard imaging method for the pretreatment and follow-up evaluation of GISTs. Several studies have investigated the predictive value of multiple CT findings for the malignant potential of GISTs[13,29-31]. The results varied, possibly due to the different inclusion criteria and subjective assessment standards. A previous study noted that CT findings were predictors of risk stratification for GISTs[29]. In this study, univariate analyses revealed that high-grade malignant potential tumors tended to have an irregular shape, indistinct tumor margins, necrosis, and ulceration, consistent with previous studies[30,32]. Our results also showed that high-grade malignant potential tumors frequently displayed tumors with a larger size. Tateishi *et al*[33] reported that an extrinsic epicenter and an unclear border were the most significant predictors for high-grade tumors, according to multiple stepwise logistic regression analysis. In our series, tumor size, shape, margins, the presence

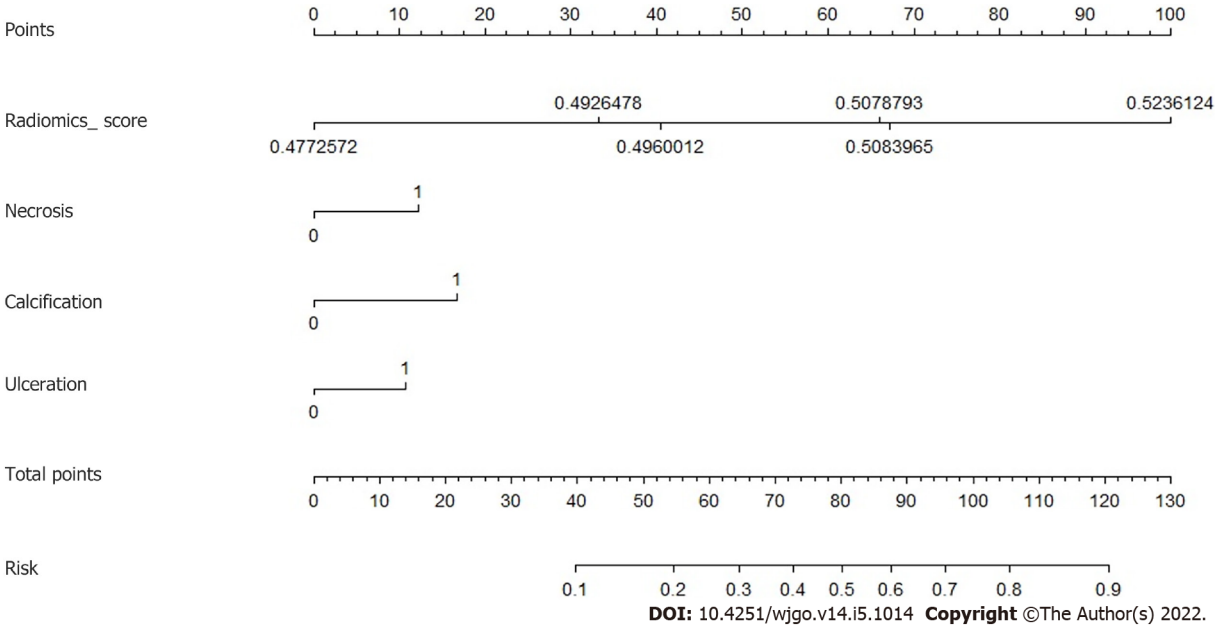

DOI: 10.4251/wjgo.v14.i5.1014 **Copyright** ©The Author(s) 2022.

Figure 4 Nomogram for the prediction. The radiomics score was combined with three computerized tomography findings: Necrosis, calcification, and ulceration.

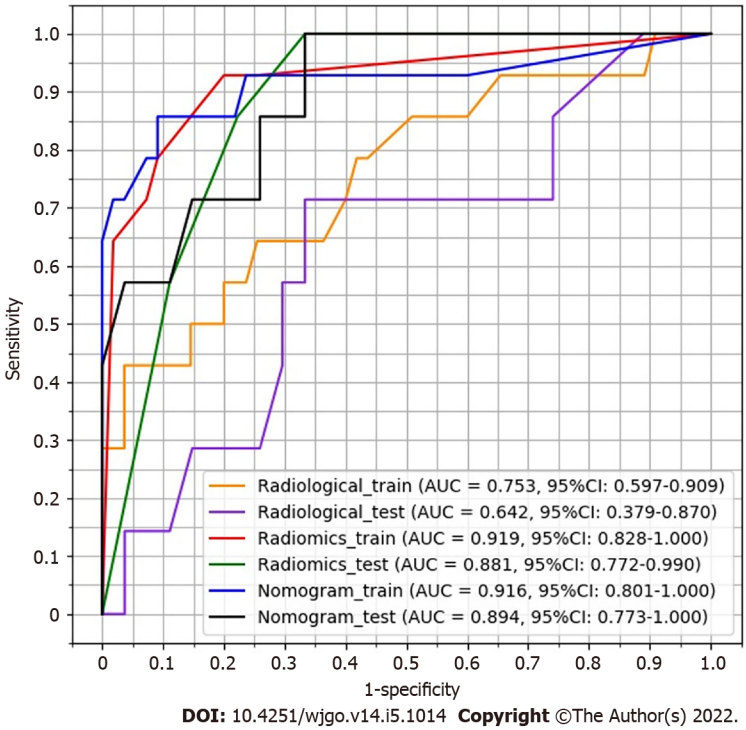

DOI: 10.4251/wjgo.v14.i5.1014 **Copyright** ©The Author(s) 2022.

Figure 5 Receiver operating characteristic curves for radiological model, radiomics model, and nomogram model. AUC: Area under the curve.

of necrosis, and ulceration were statistically significant factors for risk stratification of 2-5 cm gastric GISTs in the univariate analysis. Nevertheless, our radiological model showed that only the largest diameter and the presence of ulceration were independent predictors in backward logistic regression for high malignant potential. Limited by the inadequate predictive power of subjective CT findings, the AUC of the radiological model (0.642 for the test group) was unsatisfactory for clinical application.

Compared with subjective CT findings, both our radiomics and nomogram models had greater predictive power, as indicated by higher AUC values. Significant AUC difference was found between the radiological model and nomogram model despite a small test sample. This demonstrated that our radiomics approach with quantitative analysis had an advantage over the subjective CT findings. Unlike the radiomics models proposed by Chen *et al*[21], this study focused on the GISTs with the largest

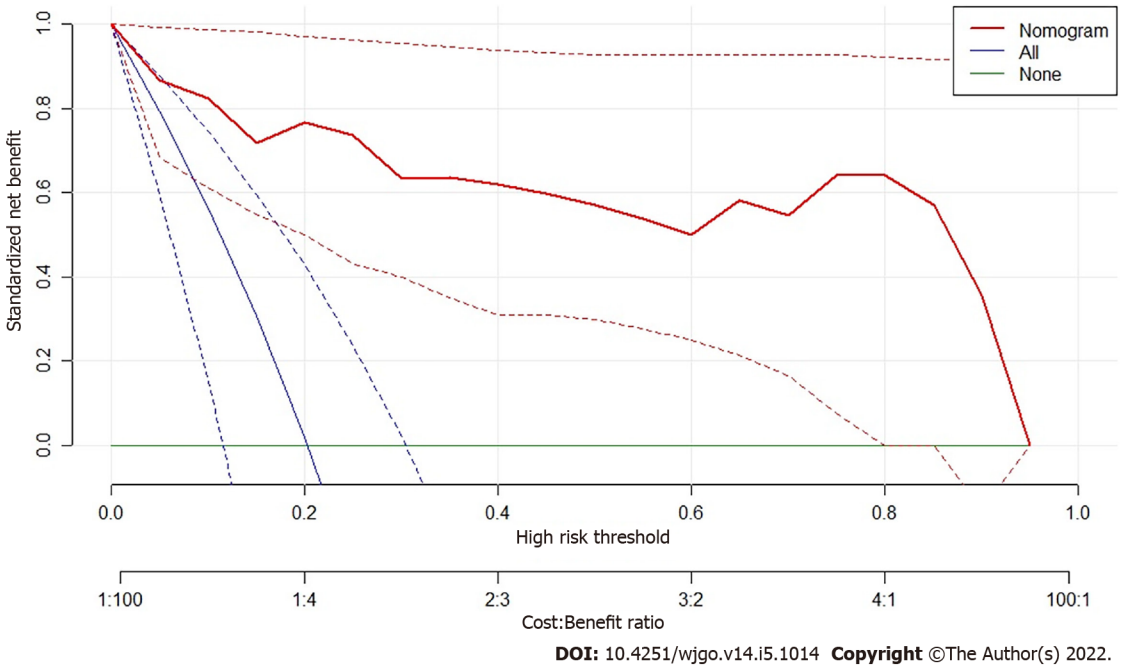

DOI: 10.4251/wjgo.v14.i5.1014

Figure 6 Decision curve of analysis. The nomogram model produces increased benefit in the whole range of risk thresholds.

diameter of 2-5 cm. According to the modified NIH criteria, the risk stratification of gastric GISTs is mainly based on the size of the tumor and mitotic count. GISTs larger than 5 cm tend to be classified into the high-risk group. It is more challenging to predict the potential risk of smaller GISTs. Therefore, it is clinically important to construct a prediction model, especially for the 2-5 cm GISTs. In this study, the ground truth of risk was determined only by mitotic counts. Mitotic counts > 5/50 HPFs were categorized into high-grade malignant potential, and mitotic counts < 5/50 HPFs were categorized into low-grade malignant potential. Therefore, the impact of tumor size was excluded, which was reasonable because 2-5 cm GISTs tended to have a uniform tumor size. In this study, although the largest diameter showed a significant difference in *t*-test examination and was included in the radiological mode, the CT findings were not selected in the final nomogram model. This indicated that tumor size was not crucial for predicting the potential risk for 2-5 cm GISTs . It is possible that manual measurement of 2-5 cm GISTs on CT images was relatively unstable compared with the quantitative features from radiomics models.

In the radiomics model, four features were selected to construct the decision trees by XGboost. The feature with the largest importance showed the gray level nonuniformity from the gray-level size zone matrix. It was used as the root node for both two decision trees. A gray-level zone was defined as the number of connected voxels that share the same gray level intensity. Gray level nonuniformity measures the variability of gray-level intensity values in the image, with a lower value indicating more homogeneity in intensity values. Therefore, signal inhomogeneity inside the tumor region in the arterial phase of CT images is important for predicting the potential risk 2-5 cm GISTs. Due to the small training samples, only four features and two trees with a depth of 2 were included in the radiomics model to avoid overfitting. The similar accuracy between the training and test group indicated a good fitting for both radiomics and nomogram models. In the nomogram, three CT findings were combined with the radiomics score to calculate the risk. This provides a simple way to incorporate the subjective findings with the result of machine learning. Although the presence of calcification was not selected in the *t*-test or logistic regression, it appeared useful in the nomogram. Probably, the mutual effect of calcification and radiomics score contributed to the improvement of the prediction accuracy.

This study had some limitations. First, our data were collected retrospectively, so further prospective research was needed. Second, this study was a single-center study. Although two scanners were used, the scanning parameters were the same. Third, a relatively small sample size limited the complexity of machine learning models. In addition, we did not have information on whether the patients experienced recurrence or death due to the lack of long-term follow-up. Nevertheless, to the best of our knowledge, this was the first study that predicted the malignant potential of 2-5 cm gastric GISTs patients by radiomics. More cohort validation and more integrable factors such as KIT and PDGFRA mutations should be considered in future research[3,34].

CONCLUSION

In this study, we developed a radiomics model and a nomogram to predict the malignant potential of 2-5 cm gastric GISTs. The models revealed more accurate predictive power compared to subjective CT findings.

ARTICLE HIGHLIGHTS

Research background

Gastrointestinal stromal tumors (GISTs) are clinically heterogeneous with varying degrees of malignant potential. Therefore, preoperative evaluation of the biological behavior of GISTs is important for surgical decision-making. Endoscopic resection is an effective and safe treatment for gastric GISTs smaller than 2 cm. Nevertheless, whether endoscopic surgery can be used in resecting gastric GISTs between 2 and 5 cm remains controversial considering the potential risk of metastasis and recurrence. The difficulty in assessing the malignant potential of 2-5 cm gastric GISTs present challenges to surgeons.

Research motivation

Preoperative prediction of the malignant potential and prognosis of GISTs is crucial for clinical decision-making. Radiomics has also been used to preoperatively predict the malignant potential of GISTs. However, the study on 2-5 cm gastric GISTs has not yet been reported.

Research objectives

As stated above, we proposed a radiomics method for predicting the malignant potential of 2-5 cm gastric GISTs based on preoperative enhanced computerized tomography (CT) images. The method may be helpful for preoperative design of individualized treatment strategy for patients with 2-5 cm gastric GISTs.

Research methods

This was a retrospective study in which three models were constructed, including radiological model, radiomics model, and nomogram model. A radiological model was constructed based on CT findings and clinical characteristics. XGboost method was used to construct a radiomics model. Nomogram was constructed by combining the radiomics score with CT findings.

Research results

The area under the curve (AUC) of the nomogram model was significantly larger than the AUC of the radiological model in both the training group and the test group. The decision curve of analysis showed that the nomogram model produces increased benefit across the entire risk threshold range.

Research conclusions

In this study, we developed a radiomics model and a nomogram for malignancy differentiation of 2-5 cm gastric GISTs, which achieved satisfactory discrimination and had the potential to act as a reproducible imaging marker to support the decision-making support in a noninvasive and effective way.

Research perspectives

Future research should be considered on model validation and more integral factors such as KIT and PDGFRA mutations.

FOOTNOTES

Author contributions: Sun XF designed the study and was responsible for the work; Sun XF, Tang L, and Ji WY conducted data collection; Sun XF and Zhang XY conducted image measurement; Zhu HT and Li XT conducted statistical analyses; Sun XF wrote the paper; all authors edited the paper.

Supported by Beijing Hospitals Authority Ascent Plan, No. 20191103; Beijing Municipal Administration of Hospitals Clinical Medicine Development of Special Funding Support, No. ZYLX201803; Beijing Natural Science Foundation, No. Z180001 and No. Z200015; and PKU-Baidu Fund, No. 2020BD027.

Institutional review board statement: This retrospective study was approved by the Institutional Review Board of Peking University Cancer Hospital & Institute.

Informed consent statement: Patients were not required to give informed consent to the study because the analysis used anonymous clinical data that were obtained after each patient agreed to treatment by written consent.

Conflict-of-interest statement: The authors have no conflicts to declare.

Data sharing statement: The authors do not want to share the data.

Country/Territory of origin: China

ORCID number: Xue-Feng Sun 0000-0001-9910-5125; Hai-Tao Zhu 0000-0002-2058-5806; Wan-Ying Ji 0000-0002-9360-8642; Xiao-Yan Zhang 0000-0003-2700-7627; Xiao-Ting Li 0000-0003-2758-3843; Ying-Shi Sun 0000-0001-9424-1910.

S-Editor: Yan JP
L-Editor: Filipodia
P-Editor: Li X

REFERENCES

1 **Polkowski M**. Endoscopic ultrasound and endoscopic ultrasound-guided fine-needle biopsy for the diagnosis of malignant submucosal tumors. *Endoscopy* 2005; **37**: 635-645 [PMID: 16010608 DOI: 10.1055/s-2005-861422]
2 **Nishida T**, Blay JY, Hirota S, Kitagawa Y, Kang YK. The standard diagnosis, treatment, and follow-up of gastrointestinal stromal tumors based on guidelines. *Gastric Cancer* 2016; **19**: 3-14 [PMID: 26276366 DOI: 10.1007/s10120-015-0526-8]
3 **Joensuu H**, Hohenberger P, Corless CL. Gastrointestinal stromal tumour. *Lancet* 2013; **382**: 973-983 [PMID: 23623056 DOI: 10.1016/S0140-6736(13)60106-3]
4 **Corless CL**, Barnett CM, Heinrich MC. Gastrointestinal stromal tumours: origin and molecular oncology. *Nat Rev Cancer* 2011; **11**: 865-878 [PMID: 22089421 DOI: 10.1038/nrc3143]
5 **Nishida T**, Kawai N, Yamaguchi S, Nishida Y. Submucosal tumors: comprehensive guide for the diagnosis and therapy of gastrointestinal submucosal tumors. *Dig Endosc* 2013; **25**: 479-489 [PMID: 23902569 DOI: 10.1111/den.12149]
6 **An W**, Sun PB, Gao J, Jiang F, Liu F, Chen J, Wang D, Li ZS, Shi XG. Endoscopic submucosal dissection for gastric gastrointestinal stromal tumors: a retrospective cohort study. *Surg Endosc* 2017; **31**: 4522-4531 [PMID: 28374257 DOI: 10.1007/s00464-017-5511-3]
7 **Shen C**, Chen H, Yin Y, Chen J, Han L, Zhang B, Chen Z. Endoscopic versus open resection for small gastric gastrointestinal stromal tumors: safety and outcomes. *Medicine (Baltimore)* 2015; **94**: e376 [PMID: 25569663 DOI: 10.1097/MD.0000000000000376]
8 **Andalib I**, Yeoun D, Reddy R, Xie S, Iqbal S. Endoscopic resection of gastric gastrointestinal stromal tumors originating from the muscularis propria layer in North America: methods and feasibility data. *Surg Endosc* 2018; **32**: 1787-1792 [PMID: 28916847 DOI: 10.1007/s00464-017-5862-9]
9 **Kim MY**, Park YS, Choi KD, Lee JH, Choi KS, Kim DH, Song HJ, Lee GH, Jung HY, Kim JH, Yun SC, Kim KC, Yook JH, Oh ST, Kim BS, Ryu MH, Kang YK. Predictors of recurrence after resection of small gastric gastrointestinal stromal tumors of 5 cm or less. *J Clin Gastroenterol* 2012; **46**: 130-137 [PMID: 21617541 DOI: 10.1097/MCG.0b013e31821f8bf6]
10 **Miettinen M**, Lasota J. Gastrointestinal stromal tumors: pathology and prognosis at different sites. *Semin Diagn Pathol* 2006; **23**: 70-83 [PMID: 17193820 DOI: 10.1053/j.semdp.2006.09.001]
11 **Joensuu H**. Risk stratification of patients diagnosed with gastrointestinal stromal tumor. *Hum Pathol* 2008; **39**: 1411-1419 [PMID: 18774375 DOI: 10.1016/j.humpath.2008.06.025]
12 **von Mehren M**, Randall RL, Benjamin RS, Boles S, Bui MM, Ganjoo KN, George S, Gonzalez RJ, Heslin MJ, Kane JM, Keedy V, Kim E, Koon H, Mayerson J, McCarter M, McGarry SV, Meyer C, Morris ZS, O'Donnell RJ, Pappo AS, Paz IB, Petersen IA, Pfeifer JD, Riedel RF, Ruo B, Schuetze S, Tap WD, Wayne JD, Bergman MA, Scavone JL. Soft Tissue Sarcoma, Version 2.2018, NCCN Clinical Practice Guidelines in Oncology. *J Natl Compr Canc Netw* 2018; **16**: 536-563 [PMID: 29752328 DOI: 10.6004/jnccn.2018.0025]
13 **Chen T**, Xu L, Dong X, Li Y, Yu J, Xiong W, Li G. The roles of CT and EUS in the preoperative evaluation of gastric gastrointestinal stromal tumors larger than 2 cm. *Eur Radiol* 2019; **29**: 2481-2489 [PMID: 30617491 DOI: 10.1007/s00330-018-5945-6]
14 **Nishida T**, Sakai Y, Takagi M, Ozaka M, Kitagawa Y, Kurokawa Y, Masuzawa T, Naito Y, Kagimura T, Hirota S; members of the STAR ReGISTry Study Group. Adherence to the guidelines and the pathological diagnosis of high-risk gastrointestinal stromal tumors in the real world. *Gastric Cancer* 2020; **23**: 118-125 [PMID: 31041650 DOI: 10.1007/s10120-019-00966-4]
15 **Ren C**, Wang S, Zhang S. Development and validation of a nomogram based on CT images and 3D texture analysis for preoperative prediction of the malignant potential in gastrointestinal stromal tumors. *Cancer Imaging* 2020; **20**: 5 [PMID: 31931874 DOI: 10.1186/s40644-019-0284-7]
16 **Hodgdon T**, McInnes MD, Schieda N, Flood TA, Lamb L, Thornhill RE. Can Quantitative CT Texture Analysis be Used

to Differentiate Fat-poor Renal Angiomyolipoma from Renal Cell Carcinoma on Unenhanced CT Images? *Radiology* 2015; **276**: 787-796 [PMID: 25906183 DOI: 10.1148/radiol.2015142215]

17 **Lambin P**, Rios-Velazquez E, Leijenaar R, Carvalho S, van Stiphout RG, Granton P, Zegers CM, Gillies R, Boellard R, Dekker A, Aerts HJ. Radiomics: extracting more information from medical images using advanced feature analysis. *Eur J Cancer* 2012; **48**: 441-446 [PMID: 22257792 DOI: 10.1016/j.ejca.2011.11.036]

18 **Gillies RJ**, Kinahan PE, Hricak H. Radiomics: Images Are More than Pictures, They Are Data. *Radiology* 2016; **278**: 563-577 [PMID: 26579733 DOI: 10.1148/radiol.2015151169]

19 **Wu S**, Zheng J, Li Y, Yu H, Shi S, Xie W, Liu H, Su Y, Huang J, Lin T. A Radiomics Nomogram for the Preoperative Prediction of Lymph Node Metastasis in Bladder Cancer. *Clin Cancer Res* 2017; **23**: 6904-6911 [PMID: 28874414 DOI: 10.1158/1078-0432.CCR-17-1510]

20 **Huang YQ**, Liang CH, He L, Tian J, Liang CS, Chen X, Ma ZL, Liu ZY. Development and Validation of a Radiomics Nomogram for Preoperative Prediction of Lymph Node Metastasis in Colorectal Cancer. *J Clin Oncol* 2016; **34**: 2157-2164 [PMID: 27138577 DOI: 10.1200/JCO.2015.65.9128]

21 **Chen T**, Ning Z, Xu L, Feng X, Han S, Roth HR, Xiong W, Zhao X, Hu Y, Liu H, Yu J, Zhang Y, Li Y, Xu Y, Mori K, Li G. Radiomics nomogram for predicting the malignant potential of gastrointestinal stromal tumours preoperatively. *Eur Radiol* 2019; **29**: 1074-1082 [PMID: 30116959 DOI: 10.1007/s00330-018-5629-2]

22 **von Mehren M**, Joensuu H. Gastrointestinal Stromal Tumors. *J Clin Oncol* 2018; **36**: 136-143 [PMID: 29220298 DOI: 10.1200/JCO.2017.74.9705]

23 **Singer S**, Rubin BP, Lux ML, Chen CJ, Demetri GD, Fletcher CD, Fletcher JA. Prognostic value of KIT mutation type, mitotic activity, and histologic subtype in gastrointestinal stromal tumors. *J Clin Oncol* 2002; **20**: 3898-3905 [PMID: 12228211 DOI: 10.1200/JCO.2002.03.095]

24 **Lennartsson J**, Jelacic T, Linnekin D, Shivakrupa R. Normal and oncogenic forms of the receptor tyrosine kinase kit. *Stem Cells* 2005; **23**: 16-43 [PMID: 15625120 DOI: 10.1634/stemcells.2004-0117]

25 **Blay JY**, Levard A. Adjuvant imatinib treatment in gastrointestinal stromal tumor: which risk stratification criteria and for how long? *Anticancer Drugs* 2016; **27**: 71-75 [PMID: 26457546 DOI: 10.1097/CAD.0000000000000286]

26 **Rutkowski P**, Przybył J, Zdzienicki M. Extended adjuvant therapy with imatinib in patients with gastrointestinal stromal tumors : recommendations for patient selection, risk assessment, and molecular response monitoring. *Mol Diagn Ther* 2013; **17**: 9-19 [PMID: 23355099 DOI: 10.1007/s40291-013-0018-7]

27 **Blay JY**, Rutkowski P. Adherence to imatinib therapy in patients with gastrointestinal stromal tumors. *Cancer Treat Rev* 2014; **40**: 242-247 [PMID: 23931926 DOI: 10.1016/j.ctrv.2013.07.005]

28 **López RL**, del Muro XG. Management of localized gastrointestinal stromal tumors and adjuvant therapy with imatinib. *Anticancer Drugs* 2012; **23** Suppl: S3-S6 [PMID: 22739667 DOI: 10.1097/CAD.0b013e3283559fab]

29 **Zhou C**, Duan X, Zhang X, Hu H, Wang D, Shen J. Predictive features of CT for risk stratifications in patients with primary gastrointestinal stromal tumour. *Eur Radiol* 2016; **26**: 3086-3093 [PMID: 26699371 DOI: 10.1007/s00330-015-4172-7]

30 **Kim HC**, Lee JM, Kim KW, Park SH, Kim SH, Lee JY, Han JK, Choi BI. Gastrointestinal stromal tumors of the stomach: CT findings and prediction of malignancy. *AJR Am J Roentgenol* 2004; **183**: 893-898 [PMID: 15385278 DOI: 10.2214/ajr.183.4.1830893]

31 **Mazzei MA**, Cioffi Squitieri N, Vindigni C, Guerrini S, Gentili F, Sadotti G, Mercuri P, Righi L, Lucii G, Mazzei FG, Marrelli D, Volterrani L. Gastrointestinal stromal tumors (GIST): a proposal of a "CT-based predictive model of Miettinen index" in predicting the risk of malignancy. *Abdom Radiol (NY)* 2020; **45**: 2989-2996 [PMID: 31506758 DOI: 10.1007/s00261-019-02209-7]

32 **Burkill GJ**, Badran M, Al-Muderis O, Meirion Thomas J, Judson IR, Fisher C, Moskovic EC. Malignant gastrointestinal stromal tumor: distribution, imaging features, and pattern of metastatic spread. *Radiology* 2003; **226**: 527-532 [PMID: 12563150 DOI: 10.1148/radiol.2262011880]

33 **Tateishi U**, Hasegawa T, Satake M, Moriyama N. Gastrointestinal stromal tumor. Correlation of computed tomography findings with tumor grade and mortality. *J Comput Assist Tomogr* 2003; **27**: 792-798 [PMID: 14501372 DOI: 10.1097/00004728-200309000-00018]

34 **Joensuu H**, Wardelmann E, Sihto H, Eriksson M, Sundby Hall K, Reichardt A, Hartmann JT, Pink D, Cameron S, Hohenberger P, Al-Batran SE, Schlemmer M, Bauer S, Nilsson B, Kallio R, Junnila J, Vehtari A, Reichardt P. Effect of KIT and PDGFRA Mutations on Survival in Patients With Gastrointestinal Stromal Tumors Treated With Adjuvant Imatinib: An Exploratory Analysis of a Randomized Clinical Trial. *JAMA Oncol* 2017; **3**: 602-609 [PMID: 28334365 DOI: 10.1001/jamaoncol.2016.5751]

Published by **Baishideng Publishing Group Inc**
7041 Koll Center Parkway, Suite 160, Pleasanton, CA 94566, USA
Telephone: +1-925-3991568
E-mail: bpgoffice@wjgnet.com
Help Desk: https://www.f6publishing.com/helpdesk
https://www.wjgnet.com